# START-TO-END SIMULATIONS OF THE ENERGY RECOVERY LINAC PROTOTYPE FEL

C. Gerth*, M. Bowler, B. Muratori, H.L. Owen, N.R. Thompson,
ASTeC, Daresbury Laboratory, Warrington WA4 4AD, UK
B. Faatz, DESY, Notkestraße 85, D-22603 Hamburg, Germany
B.W.J. McNeil, University of Strathclyde, Glasgow, G2 0NG, Scotland

*Abstract*

Daresbury Laboratory is currently building an Energy Recovery Linac Prototype (ERLP) that serves as a testbed for the study of beam dynamics and accelerator technology important for the design and construction of the proposed 4th Generation Light Source project. Two major objectives of the ERLP are the demonstration of energy recovery and of energy recovery from a beam disrupted by an FEL interaction as supplied by an infrared oscillator system. In this paper we present start-to-end simulations of the ERLP including such an FEL interaction. The beam dynamics in the high-brightness injector, which consists of a DC photocathode gun and a super-conducting booster, have been modelled using the particle tracking code ASTRA. After the booster, particles have been tracked with the code elegant. The 3D code GENESIS 1.3 was used to model the FEL interaction with the electron beam.

## INTRODUCTION

The performance of a free-electron laser (FEL) depends crucially on the electron beam parameters. While analytical calculations can give an estimate of the expected performance, numerical start-to-end (S2E) simulations are required to account for various aspects of beam dynamics during the generation, transport and compression of the beam [1, 2, 3]. FELs based on the Energy Recovery Linac (ERL) concept have a distinct advantage in terms of rf power and beam dump requirements. However, another aspect becomes important for S2E simulations: the electron beam, which may have a large energy spread induced by the FEL process, needs to be recirculated for deceleration and then transported into the beam dump [4].

Daresbury Laboratory are currently building an ERL Prototype [5] which will operate at a beam energy of 35 MeV and drive an infra-red oscillator FEL. In this paper we present the results of the first S2E simulations for the ERLP including the FEL. To account for space charge effects, ASTRA [6] was used for the modelling of the low energy part (350 keV) of the injector from the cathode to the booster. The beam was tracked with elegant [7] from the booster (8.35 MeV) to the main linac (35 MeV) and then to the FEL. The FEL interaction was modelled with GENESIS, and elegant was used to transport the beam back to the linac for energy recovery and then to the beam dump.

* c.gerth@dl.ac.uk

## INJECTOR

The injector consists of a high-average current DC photocathode gun, a booster and a transfer line to the main linac. The DC photocathode gun is a replica of the 500 kV Jefferson Lab gun [8] and will operate at a nominal accelerating voltage of 350 kV and bunch charge of 80 pC. Electrons will be generated at a GaAs photocathode by the frequency-doubled light (532 nm) of a mode-locked Nd:$YVO_4$ laser with an oscillator frequency of 81.25 MHz. Two solenoids will be used for transverse focusing and emittance compensation, and a normal-conducting single-cell buncher cavity will be utilised to decrease the bunch length from the GaAs cathode. The buncher cavity will be operated at 1.3 GHz and is based on the buncher design employed at the ELBE facility [9]. Electrons are accelerated to an energy of 8.35 MeV in the booster, which consists of two super-conducting 9-cell TESLA-type cavities operated at 1.3 GHz. The cryo-module design is based on the design of the ELBE linac [10]. The layout of the ERLP injector is shown in Fig. 1 and a detailed description of the injector design can be found in Ref. [11].

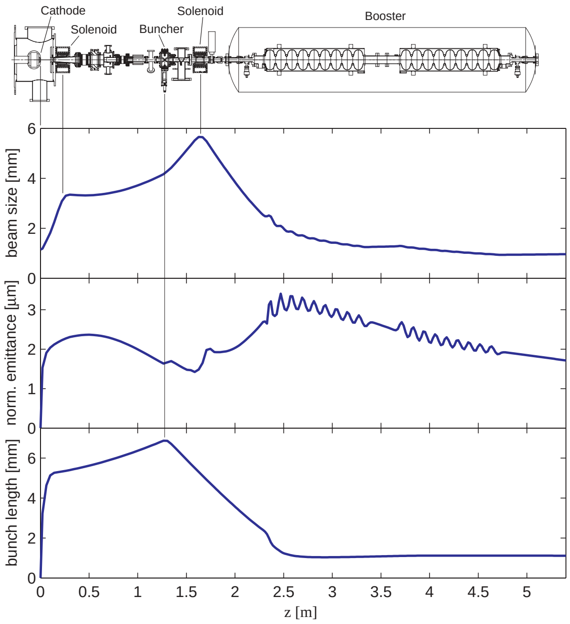


Figure 1: Layout of the ERLP injector and evolution of the beam size, norm. emittance and bunch length (all rms).

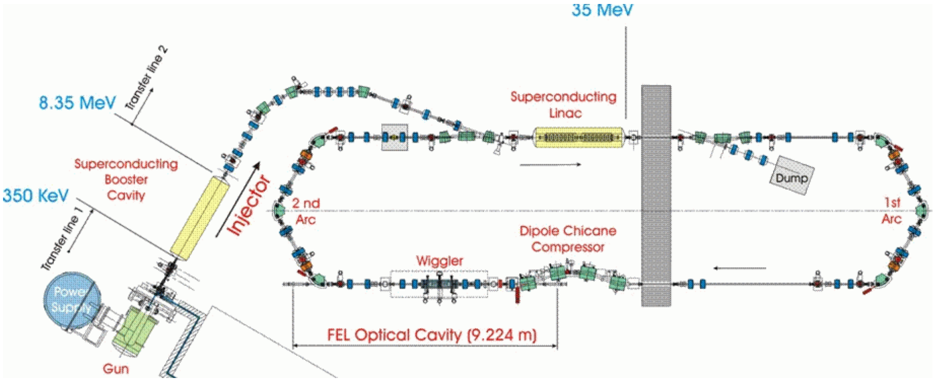


Figure 2: The layout of the ERL Prototype.

To account for space charge effects in the injector the particle tracking code ASTRA has been used for the modelling of the beam dynamics. The transverse properties of the electron bunch at the cathode are determined by the cathode laser parameters whereas the longitudinal profile is dominated by the GaAs cathode for short laser pulses due to the rather long response time of GaAs. For the modelling, a longitudinal Gaussian distribution with an rms length of 20 ps has been assumed. The transverse distribution was chosen to be Gaussian with an rms beam size $\sigma_r$ = 1.25 mm truncated at $\pm 2\sigma_r$. Results for the evolution of the rms values of the beam size, normalised emittance and bunch length are shown in Fig. 1 for a simulation with 250k macro-particles.

The booster is followed by a transfer line which transports the beam to the straight of the main linac where it is merged with the full energy (35 MeV) single-pass recirculated beam. The transfer line employs four quadrupoles to match the beam into a double-bend achromat which is followed by a 2-dipole achromatic dog-leg. Tracking the beam from the booster to the main linac was carried out by the code elegant. This code does not include space charge effects and so the resulting emittance degradation, as studied in [12], have been simulated further upstream by using appropriate rf phase and sextupole settings.

## BEAM TRANSPORT SYSTEM

The layout of the ERLP is shown in Fig. 2. Electrons from the injector are accelerated to 35 MeV in the superconducting main linac, which is identical to the booster and composed of two 9-cell TESLA-type cavities. Two 180° triple-bend achromat (TBA) arcs [13] are used to recirculate the beam to the main linac where the electrons are decelerated to their injection energy. The electrons are separated from the full energy beam (35 MeV) by an extraction chicane and then dumped in the beam dump. A 4-dipole chicane provides bunch compression upstream of the wiggler and bypasses one of the FEL mirrors.

The minimum bunch length is required within the wiggler. The compression chicane has a static $R_{56}^{C}$ of 0.28 m (positive in our sign convention) [14]. For optimum bunch compression, the main linac needs to be operated at an off-crest phase of about $\varphi_{\rm rf} \simeq 9°$. The TBA arcs are able to provide a large negative $R_{56}$. In nominal setup, the first arc is set to $R_{56}^{A1} = 0$ whereas the second arc is tuned to $R_{56}^{A2} = -R_{56}^{C}$ in order to decompress the bunch. The sextupoles in the first arc can be used to linearise the lowest-order curvature induced by the sinusoidal rf during acceleration by varying $T_{566}$. The effect of the sextupoles on the longitudinal phase space is demonstrated in Figure 3. Two cases are compared: all sextupoles turned off and all sextupoles excited to 100 m$^{-3}$. The sextupoles in the second arc can be used to minimise the energy spread after deceleration for optimised energy recovery and extraction to the beam dump.

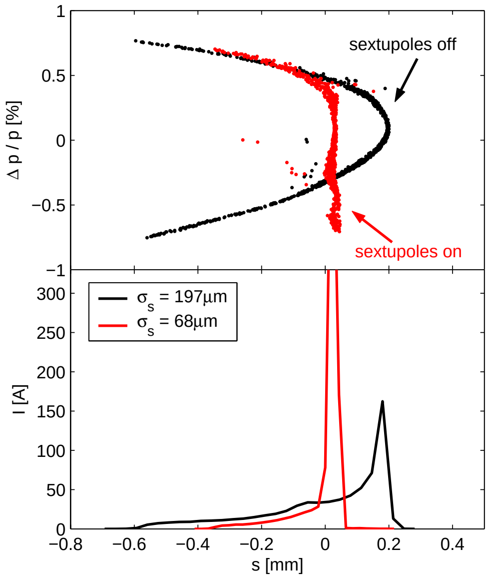


Figure 3: Comparison of longitudinal phase space after the compressor chicane with sextupoles turned on and off.

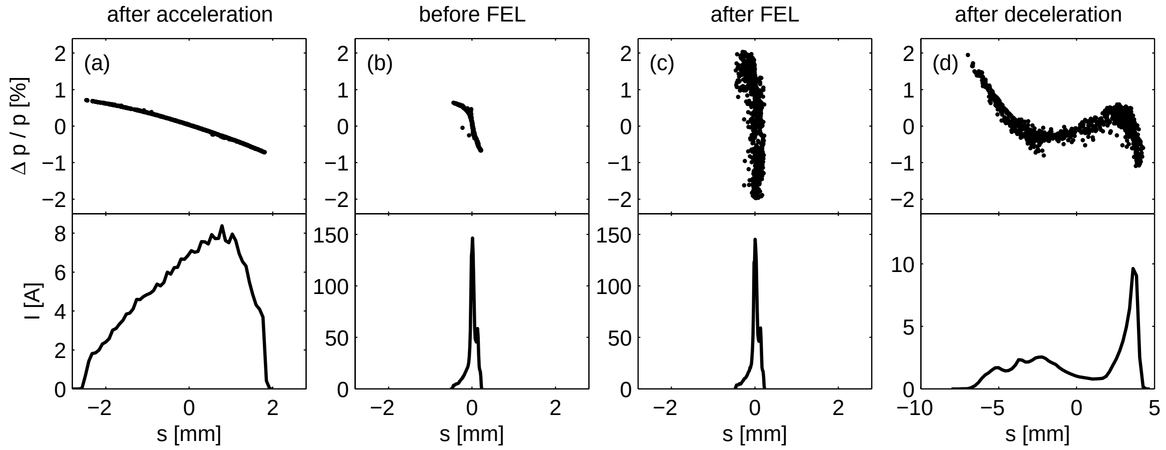


Figure 4: Longitudinal phase space and bunch profile at different locations in the ERLP: (a) after off-crest acceleration by $\varphi_{\rm rf} = 7.8°$ in the main linac; (b) after the compressor chicane with the sextupoles set to 120 $\rm m^{-3}$; (c) after FEL interaction; (d) after energy recovery in the main linac.

Results of the S2E simulations for the longitudinal phase space and bunch profile at 4 different locations in the ERLP are shown in Fig. 4: (a) after acceleration in the main linac, (b) after the compression chicane, (c) after the FEL, and (d) after deceleration. The ASTRA particle distribution from the injector modelling was used as an input for elegant, and the beam was tracked from the exit of the booster to the wiggler; the program MAD8 was used to match the lattice functions. The bunch was not fully compressed in the S2E simulation (Fig. 4(b)). The rf phase $\varphi_{\rm rf}$ and sextupole settings have been chosen to approximate the expected beam parameters at the wiggler enterance, thus simulating the effects of the neglected space charge in the injector to linac beamline. The FEL interaction, which induces a large energy spread as can be seen in Fig. 4(c), was modelled with GENESIS 1.3 and is described in more detail in the next section. The particle distribution was then converted back to elegant and tracked to the beam dump. When the second arc is set to $R_{56}^{A2} = -R_{56}^{C}$, the deceleration phase is given by $\varphi_{\rm rf} + \pi$. In order to achieve exactly the injection energy during deceleration, the deceleration phase needs to be reduced slightly to account for the mean energy loss of about 0.8% in the FEL process. Apertures were included in the elegant tracking, which were chosen to be 10% smaller than the envisaged vacuum chamber dimensions to approximately account for the effect of misalignment. No particles were lost during the recirculation even with the sextupoles turned off in the second arc.

## FEL

The wiggler has been supplied on loan from Jefferson Laboratory, and is a planar device with 40 periods of length 27 mm. The magnet arrays are vertical giving focussing in the horizontal plane. The matched beam conditions in transverse phase space are therefore a waist in the horizontal plane at the entrance to the wiggler and a waist in the vertical plane at the centre of the wiggler. The desired $\beta$-function at the wiggler entrance in the horizontal plane is 0.5 m. In the vertical plane the $\alpha$ and $\beta$ values are set to give a waist in the centre of the wiggler with the minimal vertical beam radius averaged along the wiggler. The optimum matched beam parameters at the wiggler entrance were found to be $\alpha_y$ = 1.75 and $\beta_y$ = 1.25 m.

The shortest possible length of the optical cavity, defined by the bunch repetition frequency and layout constraints, is $D$ = 9.22 m. The wiggler is positioned slightly off-centre within the cavity, and the mirror radii of curvature $R_1$ and $R_2$ are chosen to give a near-concentric cavity with an optical waist in the centre of the wiggler. The Rayleigh length is 0.75 m compared to a wiggler length of 1.08 m – the optimum Rayleigh length for FEL coupling would be less than this but would drive the cavity towards instability. The cavity stability is given by $g_1 \cdot g_2 = 0.9$, with $g_1 = 1 - D/R_1$ and $g_2 = 1 - D/R_2$.

The FEL process was modelled with GENESIS as follows: first, the projected rms values of the tracked particle distribution were calculated, and the predicted performance of the FEL was estimated with analytical formulae and GENESIS in steady-state mode (FEL wavelength, intracavity power, etc.). These results and the SDDS toolkit program elegant2genesis were then used to generate the input files for GENESIS, which was run in time-dependent mode with a seed power given by the analytic estimate of the intra-cavity peak power at saturation of ≈80 MW. This seed power is approximated by a uniform intensity over the entire electron bunch. Although this is not an exact representation of the pulse structure in a cavity it should approximate reasonably well the energy spread induced by the FEL interaction.

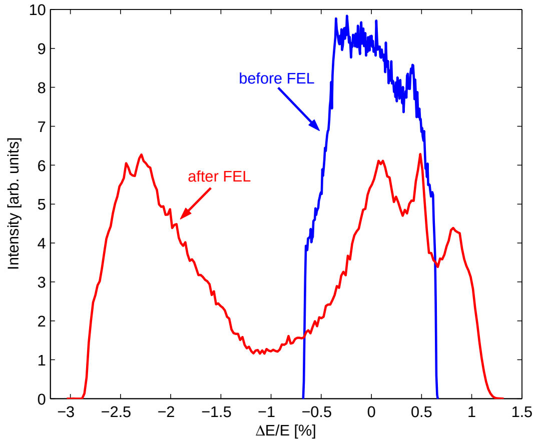


Figure 5: Results of GENESIS simulation: energy spread induced by the FEL interaction with 80 MW seed beam (data taken from Figs. 4(b) and (c)).

The utility code elegant2genesis discretises the elegant supplied macro-particle distribution into radiation wavelength slices (here 4.4 $\mu$m) and calculates the relevant GENESIS input parameters. The charge of each slice is proportional to the number of macro particles it contains. These parameters are then applied to form a GENESIS macro-particle distribution with a constant number of particles for each slice (typically 8192). To convert the GENESIS output file back to an elegant input file, the number of particles in each slice should again be made proportional to the slice charge. This is achieved by randomly sampling the GENESIS particles to give the required number of elegant macro particles.

Care should be taken when converting complex particle distributions using elegant2genesis. Inhomogeneous distributions may be inadvertently simplified as elegant2genesis only calculates the mean and rms values for each slice. For instance, in the 'sextupoles-off' particle distribution of Fig. 3, the tail of the distribution comprises two energy bands each of which has a relatively small energy spread. The calculation of the slice values by elegant2genesis results in a mean energy in the centre with a rather large energy spread. This situation does not arise for the 'sextupoles-on' particle distribution used here in the S2E simulation.

The energy profiles of the electron bunch before and after the FEL process are compared in Fig. 5 for a seed power of 80 MW. The mean energy loss in the simulation is 0.8% which is in good agreement with analytical predictions. The return arc must have an energy acceptance sufficient to transport all the electrons. Assuming a Gaussian distribution, a range of $\pm 3\sigma_E$ represents 99.7% of the electrons, so an estimate of the full FEL exhaust energy spread is given by $6\sigma_E$. A full energy spread of $\approx$ 4% is predicted by one-dimensional steady-state codes for the given parameters which is in good agreement with the GENESIS result shown in Fig. 5.

## SUMMARY AND OUTLOOK

First S2E simulations of an ERL including both an FEL interaction and energy recovery have been performed. The particle tracking codes ASTRA and elegant were used for particle transport. The FEL oscillator was modelled as a seeded single pass amplifier configuration with a seed power equivalent to the estimated intra-cavity peak power at saturation.

There is ongoing work to improve the S2E simulations. Space charge effects will be included in the modelling of the transfer line from the booster to the main linac at 8.35 MeV. To improve the modelling of the FEL process, a Gaussian seed pulse of variable length will be implemented. The implementation of cavity feedback effects by feeding the output radiation back into the wiggler and including cavity parameters and slippage effects are also envisaged.

## REFERENCES

[1] S. Reiche *et al.*, "Start-to-end Simulations for the LCLS Xray-FEL", PAC'01, Chicago, June 2001.

[2] M. Biagini *et al.*, "Start to End Simulations for the SPARX Proposal", PAC'03, Portland, May 2003.

[3] M. Dohlus *et al.*, "Start-To-End Simulations of SASE FEL at the TESLA Test Facility, Phase I: comparison with experimental results", Nucl. Instr. and Meth. A **528**, 448, 2004.

[4] P. Piot *et al.*, "Longitudinal phase space manipulation in energy recovering linac-driven free-electron lasers", Phys. Rev. ST-AB **6**, 030702, 2003.

[5] M.W. Poole, E.A. Seddon, "4GLS and the Prototype Energy Recovery Linac Project at Daresbury", EPAC'04, Lucerne, July 2004.

[6] K. Flöttmann, "ASTRA User Manual", September 18, 2000. `http//www.desy.de/~mpyflo`.

[7] M. Borland, "elegant: A Flexible SDDS-Compliant Code for Accelerator Simulation ", APS LS-287, September 2000.

[8] T. Siggins *et al.*, "Performance of a DC GaAs photocathode gun for the Jefferson lab FEL", Nucl. Instr. and Meth. A **475** (2001) 549.

[9] E. Wooldridge *et al.*, "Comparison of different Buncher Cavity Designs for the 4GLS ERLP", EPAC'04, Lucerne, July 2004.

[10] A. Büchner *et al.*, "The ELBE-Project at Dresden-Rossendorf", EPAC'00, Vienna, June 2000.

[11] C. Gerth, F.E. Hannon, "Injector Design for the 4GLS Energy Recovery Linac Prototype", EPAC'04, Lucerne, July 2004.

[12] B. Muratori *et al.*, "Space Charge effects for the ERL Prototype", EPAC'04, Lucerne, July 2004.

[13] H.L. Owen, B. Muratori, "Choice of Arc Design for the ERL Prototype at Daresbury Laboratory", EPAC'04, Lucerne, July 2004.

[14] B. Muratori *et al.*, "Optics Layout for the ERL Prototype at Daresbury Laboratory ", EPAC'04, Lucerne, July 2004.